# Polylactide/Nano and Microscale Silica Composite Films. I. Preparation and Characterization

**Jiann-Wen Huang,[1] Yung Chang Hung,[2] Ya-Lan Wen,[3] Chiun-Chia Kang,[4] Mou-Yung Yeh[2,5]**

[1]*Department of Styling and Cosmetology, Tainan University of Technology, Yung Kang City, 710 Taiwan, Republic of China*
[2]*Department of Chemistry, National Cheng Kung University, Tainan City, 701 Taiwan, Republic of China*
[3]*Department of Nursing, Meiho Institute of Technology, Pingtung, 912 Taiwan, Republic of China*
[4]*R&D Center, Hi-End Polymer Film Co., Ltd. 15-1 Sin Jhong Rd., Sin Ying City 730, Taiwan*
[5]*Sustainable Environment Research Center, National Cheng Kung University, Tainan City, 701 Taiwan, Republic of China*

Received 5 July 2008; accepted 31 October 2008
DOI 10.1002/app.29616
Published online 9 February 2009 in Wiley InterScience (www.interscience.wiley.com).

**ABSTRACT:** Polylactide (PLA)/silica composite films were prepared by two methods: blending nanoscale colloidal silica sol and sol–gel. The nano and microscale silica particles, respectively, were well dispersed in PLA when observed using scanning electron microscopy and transmission electron microscope. The mechanical and thermal stability of composite films were measured before and after hydrolysis by Instron and thermogravimetric analysis. The fillers increase tensile strength, Young's modulus, thermal stability, and hydrolysis resistance with increasing silica content. The nanoscale particles exhibit better effects than the microscale ones. The activation energy, $E_a$, of thermal decomposition is also simulated by the Kissinger and Ozawa equation. The results also show that the thermal stability is increased by the incorporation of silica particles and is lowered by hydrolysis. © 2009 Wiley Periodicals, Inc. J Appl Polym Sci 112: 1688–1694, 2009

**Key words:** polylactide; silica; composite; mechanical properties; thermal stability

## INTORDUCTION

Polylactide (PLA) is a linear aliphatic thermoplastic polyester and has obtained much attention since 1970s because of its biodegradability and friendliness to environment. It is seen as a renewable resource as it is prepared from starch via fermentation. However, its brittleness[1] and low crystallization rate[2] are major defects for many applications. PLA has been blended with biodegradable[3–5] and nonbiodegradable polymers to improve such properties.[6–12]

Nanocomposites are a class of composites in which dimensions of the reinforcing phase are in the order of nanometers.[13–16] Incorporation of nanoscale particles, especially $SiO_2$, into PLA has been shown to improve its thermal stability, melt behavior, and mechanical properties.[15,16] $SiO_2$ particles are usually prepared by a sol–gel process, which consists of two steps: hydrolysis of a metal alkoxide and polycondensation of the hydrolysis products. The process provides a chemical route to ceramics of high purity and controlled microstructure. The sol–gel technique also allows coupling with organic polymeric materials,[17,18] and nanoscale colloidal silica sol has been used in the preparation of epoxy/$SiO_2$[19] and PI/$SiO_2$.[20]

In this article, PLA/$SiO_2$ composites are prepared by a sol–gel process and blending with commercial silica sol. The dispersion of $SiO_2$ was observed, and its effect on the mechanical and thermal stability before and after hydrolytic aging. The values of apparent decomposition activation energies ($E_a$) were evaluated with kinetic method.

## EXPERIMENTAL

### Materials

PLA with a number-average molecular weight ($M_n$) of 206,000–207,000 was kindly provided by Wei Mon Industrial (Taipei, Taiwan). *N*,*N*-Dimethylacetamide (DMAc) and tetraethoxy silane (TEOS) were purchased from Merck (Darmstadt, Germany). DMAc was dried over $P_2O_5$ and distilled before use. Silica sol was purchased from Nissan Chemical (Tokyo, Japan). The commercial product of DMAC-ST, in which 20–21 wt % of silica (particle size: 10–15 nm) was dispersed in DMAc. AEROSIL 200, purchased from Degussa (Essen, German), is a silica with a primary particle size of 12 nm.

*Correspondence to:* J.-W. Huang (jw.huang@msa.hinet.net).

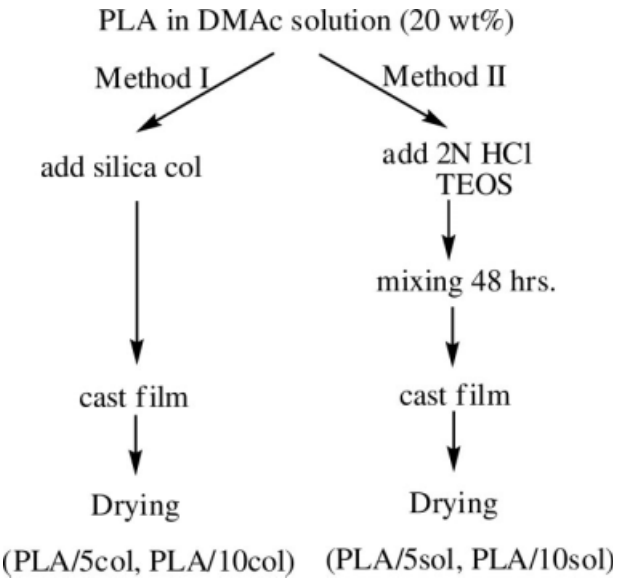


**Scheme 1** Flow chart to prepare PLA/silica composite films.

### Preparation of PLA/silica nanocomposites

The PLA solution was prepared by dissolving PLA pellets in DMAc solution with 20 wt % solid content. Two methods were used to prepare PLA/silica composite films. Method I: 5 and 10 g of silica sol (20 wt % in DMAc) were added to 100 g of PLA solution to prepare PLA/5col and PLA/10col, respectively. The blends were cast on releasing paper and dried at 30, 50, and 100°C in a vacuum oven. Method II: 1 and 2 g of TEOS were added to 100 g of PLA solution with 0.1 g of 2*N* HCl to prepare PLA/5sol and PLA/10sol, respectively. The solution was mixed at room temperature for 48 h. The blends were cast on releasing paper and dried at 30, 50, and 100°C in a vacuum oven. The thickness of dry film is ca. 70 μm. The process is shown in Scheme 1.

### Characterization

The morphologies of silica particles dispersed in PLA/silica composite films were photographed by HITACHI S-3500N scanning electron microscopy (SEM) and JEOL JEM 1200-EX transmission electron microscope (TEM). The transmittances of thin films were measured by a Shimadzu Model UV-160 spectrophotometer. FTIR spectra were recorded by a Perkin Elmer Model Spectrum One spectrometer. Hydrolytic aging was proceeded by putting samples in a aging chamber (Model HRM-80FA, Terchy Company) at 80° and 95% relative humidity. Tensile properties were tested by an Instron Instrument 4505 with a dumb-bell specimen with waist dimensions of 20 mm × 3.5 mm and at a crosshead speed of 5 mm/min. The tensile properties of each sample were determined from an average of 10 specimens. The thermal stability of the PLA and PLA/silica composite films were characterized with a Perkin Elmer TGA 6 at a heating rate of 10°C/min under nitrogen.

## RESULTS AND DISCUSSION

### Morphology

Figure 1(a,b) shows the SEM micrographs of the cross-section of PLA/5col and PLA/10/col composites, respectively, and no obvious phase separations were observed. However, PLA/5sol and PLA/10sol exhibit obvious phase separations with particle size of 0.8–1.2 and 2–3 μm, respectively. In Figure 2(a,b), the TEM was used to observe the silica dispersion in PLA/5col and PLA/10col at a higher magnification. The silica particles were dispersed homogeneously with particle size of ca. 10–20 nm.

Silica particles of different particle size can be dispersed homogeneously by both preparing methods. Blending PLA with silica sol, the silica particles remain original nanoscale size in the PLA/5col and PLA/10col without aggregation. However, microscale particles are observed in sol–gel method, and the particle sizes in PLA/5sol and PLA/10sol are dependent on the content of TEOS used. All nano and microcomposites do not exhibit debonding or holes, indicative of good interaction at the interfaces of PLA and silica.

The SEM micrograph of PLA blended directly with nanosize silica powders (AEROSIL 200) (PLA/A200) is also shown in Figure 1(e) for comparison. Aggregation and debonding are observed in PLA/A200.

Figure 3 exhibits the optical transparency of all polymer films. The nanocomposite films of PLA/5col and PLA/10col are highly transparent. The levels of transparency are similar to that of neat PLA film and not affected significantly by increasing the silica content. The dispersed phase should be smaller than the wavelengths of visible light to prevent light scattering.[21] A clear film also indicates that the size of silica phase was not greater than the wavelengths of the visible lights. It also indicates that the nanosize silica particles are well dispersed in the PLA matrix. However, the PLA/5sol and PLA/10sol display lower transparency, which may be attributed to the larger microsize silica particles.

Figure 4 shows the UV/vis transmission spectra of all polymer films. The spectra of PLA/5col and PLA/10col are close to that of neat PLA. However, the transmittance of PLA/5sol and PLA/10sol are lower at wavelength >250 nm and decreases with the increase of particle size. The PLA/A200 shows the lowest transmittance because of the aggregation of nanosize particles.

FTIR spectra of the neat and hybrid PLA films are shown in Figure 5. The characteristic absorption of

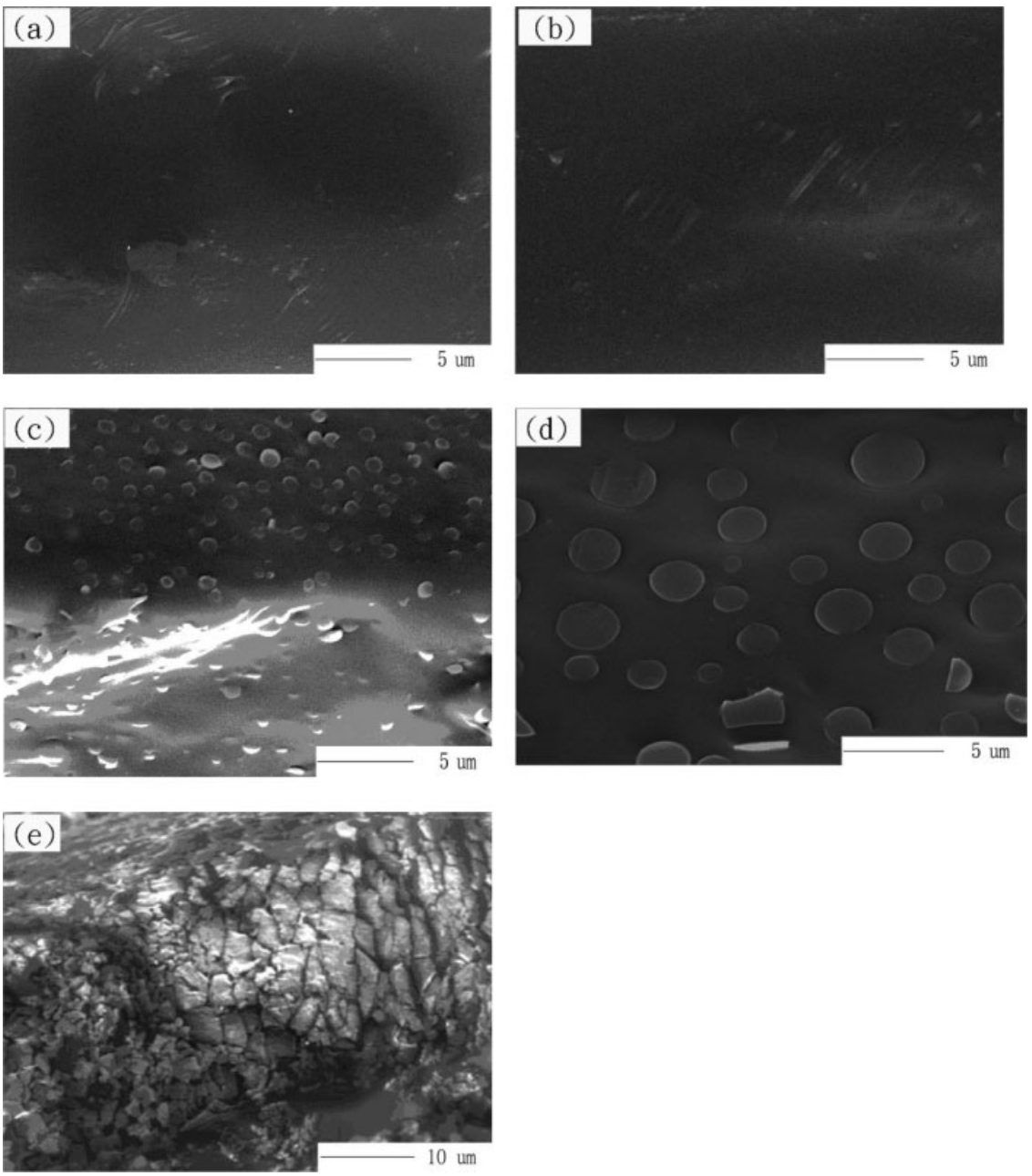


**Figure 1** SEM photographs of the PLA/silica composite films: (a) PLA/5col, (b) PLA/10col, (c) PLA/5sol, (d) PLA/5sol, and (e) PLA/A200.

PLA are 2995, 2944 $cm^{-1}$ (CH stretch), 1759 $cm^{-1}$ (C═O carbonyl), 1453, 1382, 1362 $cm^{-1}$ (CH deformation), and 1268, 1194, 1130, 1037 $cm^{-1}$ (C—O stretch).[22] The composite film shows that there are two strong absorption bands of siloxane bond, Si—O—Si, around 1090 and 450 $cm^{-1}$, which is indicative of the formation of the Si—O—Si bond.

## Mechanical properties

Figure 6(a–c) shows the stress, strain-at-break, and Young's modulus of the neat PLA and PLA/silica composite films as a function of hydrolytic degradation time. In comparison with neat PLA, an enhancement in the stress (2.6–3.5 times) and modulus (2.7–3.2 times) and increase with increasing silica content in all composite films is observed. However, the strain decreases with the addition of silica particles. The presence of the inorganic phase reduces the extent of plastic flow of the PLA phase,[23] and consequently, the strain exhibits a decreasing trend with the addition of silica particles. The filler may constrain the mobility of polymer chains in the matrix, thus affecting its modulus. The stress and modulus of PLA/silica composites with nanosize particles (PLA/5col and PLA/10col) are higher than those

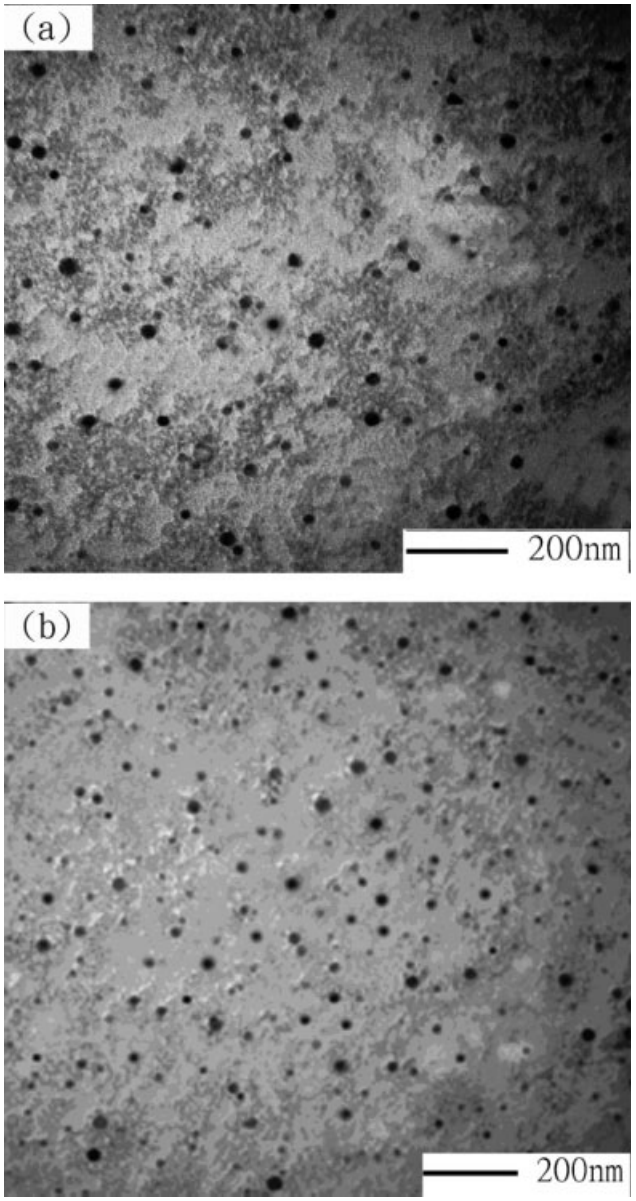


**Figure 2** TEM photographs of the PLA/silica composite films: (a) PLA/5col and (b) PLA/10col.

with microsize (PLA/5sol and PLA/10sol). It may be attributed to an increased extent of surface interaction of the inorganic phase with the PLA matrix. The results are better than PLA/layered silicate nanocomposites,[23] whose Young's modulus, yield stress, and yield strain decreases with increasing layered silicate concentration.

From Figure 6(a), it can be seen that stress of composite films remains 55–60% and 22–40% after accelerated hydrolytic aging for 24 and 48 h, respectively. In comparison with neat PLA, the tensile strength remains only at 25% and 8%. The decrease of tensile stress may be attributed to the hydrolytic cleavage of ester groups causing random chain scission and reduction of molecular weight.[24] The $M_n$ of neat

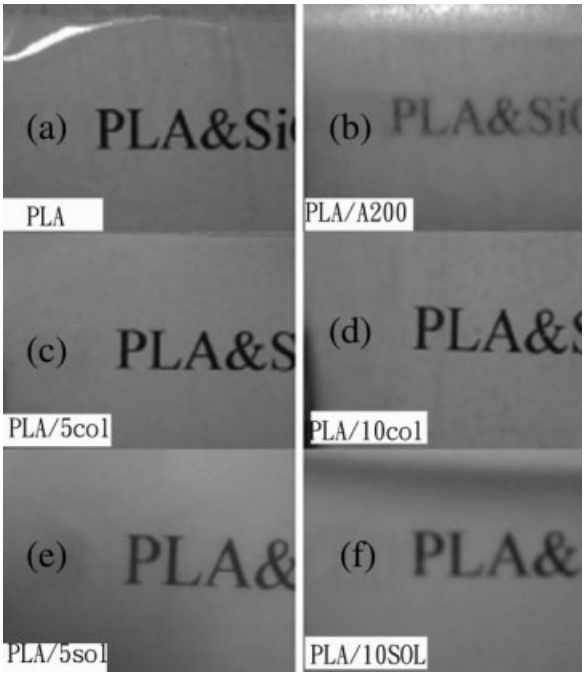


**Figure 3** Translucency of neat PLA and PLA/silica composite films.

PLA is reduced from 206,000–207,000 to 101,000 and 62,000 after hydrolytic aging for 24 and 48 h, respectively. The modulus of composite film increases slightly after the 24-h hydrolysis. It is due to a significant reduction in strain after the 24-h hydrolysis. From Figure 6(b), the presence of the inorganic phase reduces the extent of plastic flow of the PLA phase and the strain-at-break. The strain-at-break of PLA composite films decreased at an early stage of hydrolytic degradation and after that remained almost unchanged. The results are similar to literatures.[25–27]

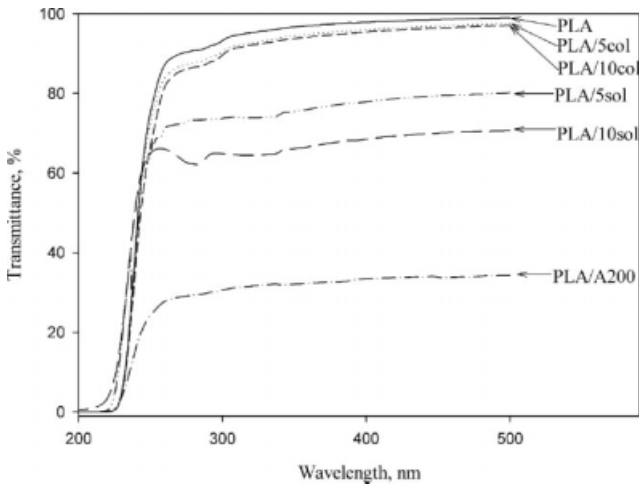


**Figure 4** UV/vis transmission spectra of neat PLA and PLA/silica composite films.

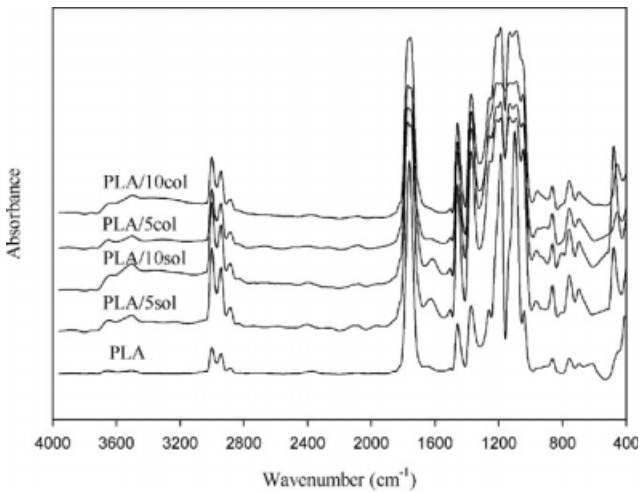


**Figure 5** FTIR spectra of neat PLA and PLA/silica composite films.

### Thermal stability

Thermal stabilities of organic materials can be improved by the introduction of inorganic components.[28] Thermogravimetric analyses (TGA) were used to monitor the effect of the silica on the thermal stability of the composites. Figure 7 shows a representative TGA analysis of PLA/10col nanocomposites.

The 5 wt % loss temperatures ($T_{5\,wt\,\%}$) for all the films are also listed in Table I. Compared with that of pure PLA, thermal stability of PLA/silica composite films increases with the addition of silica. The $T_{5\,wt\,\%}$ values of the PLA/silica composite films with nanosize particles are higher than those with microsize particles. The nanosize particles provide more surface areas to hinder molecular mobility to enhance thermal stability. The thermal behavior was contrary to PLA/clay[28–30] and PLA/nanostructured carbon nanocomposites,[31] whose thermal stability become worse with the addition of large aspect ratio of fillers (i.e., needle-like structure) result in vacant space and "chimney", and volatile components formed by thermal degradation could have readily been removed via "chimney,"[32] resulting in a rapid increase in weight loss. Further study needs to be carried out to find out the differences of thermal stability between different PLA composites.

TGA analyses show a decrease of $T_{5\,wt\,\%}$ temperature of neat PLA and all PLA/silica composites after hydrolysis (Table I). It is due to the molecular weight decrease from chain scission.

### Decomposition kinetic

Typical TGA and differential thermal analysis (DTA) curves obtained for PLA/10col at heating rate (β) of 10, 30, 50, and 70°C/min are shown in Figure 7. With increasing the heating rate from 10 to 70°C/min, the decomposition curves shifted to higher temperature. The TGA curves monotonously decreased with temperature and only a single peak observed in each DTA curve indicates a single-step degradation reaction of PLA polymer chains.

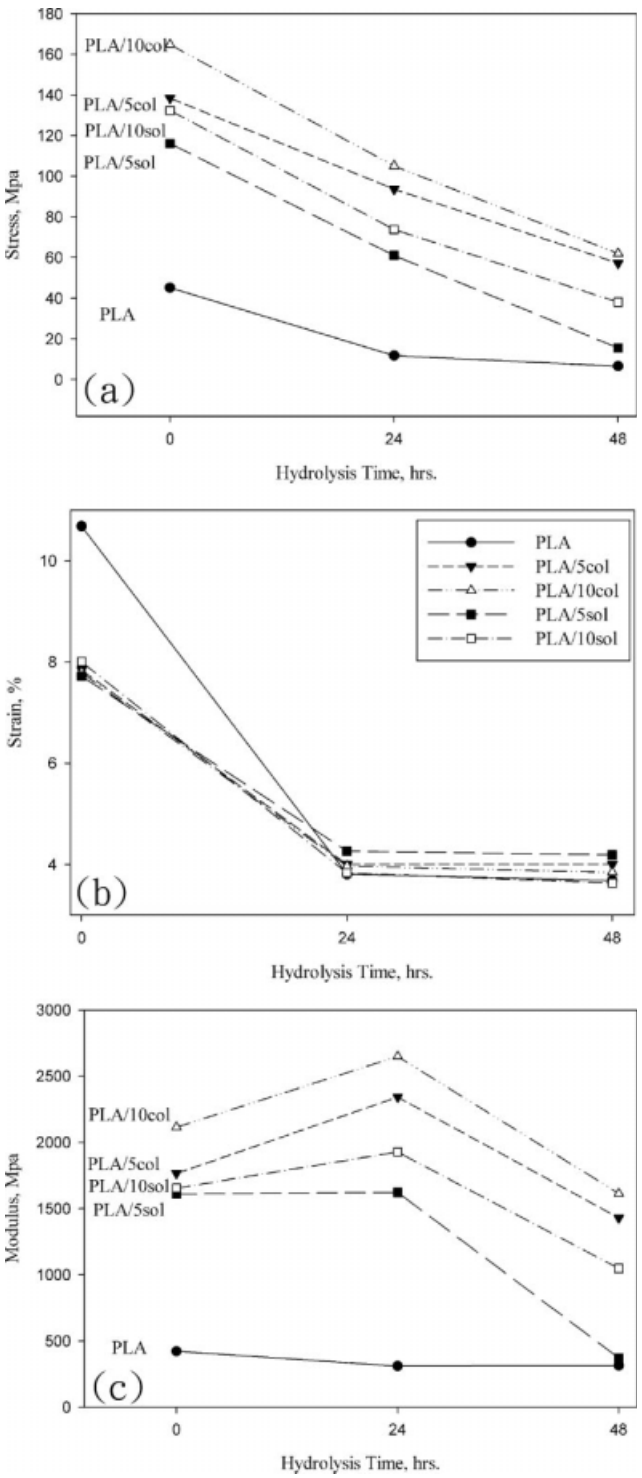


**Figure 6** Mechanical properties of neat PLA and PLA/silica composite films before and hydrolysis: (a) stress, (b) strain, and (c) modulus.

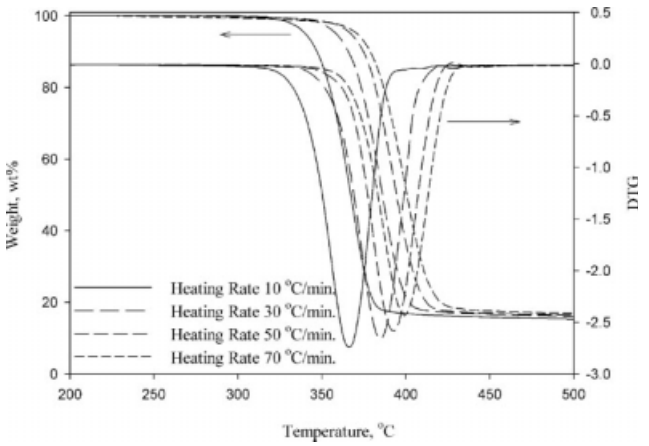


**Figure 7** TGA analysis of neat PLA and PLA/silica composite films.

The thermal degradation activation energy ($E_a$) values of the composites were determined with the Kissinger[32] and Ozawa methods.[33] The Kissinger method[32] involved the maximum weight-loss rate temperature ($T_m$) of the first-derivative weight loss curve. The Kissinger equation is shown as follows:

$$\frac{d[\ln(\beta/T_m^2)]}{d(1/T_m)} = -\frac{E_a}{R}$$

$R$ is the gas constant, the activation energy is calculated from the slope of a plot of $\ln(\beta/T_m{}^2)$ as a function of $1/T_m$, and the results are shown in Table II. The $E_a$ values are ranked as PLA/10col > PLA/5col > PLA/10sol > PLA/5col > PLA. The result is in accordance with TGA analysis. The $E_a$ values decrease after hydrolysis, which also indicate that the thermal stability becomes lower.

The Ozawa method is an approximate integral method and capable of providing activation energy data at all points on the TGA curves.[33] The expression of $E_a$ with the Ozawa method can be simplified as follows:

$$-\log\beta = 0.4567\frac{E_a}{RT}$$

**TABLE I**
**The 5 wt % Loss Temperatures ($T_{5\ wt\ \%}$) for All the Films as Prepared and after Hydrolysis**

| Hydrolysis | 0 | | | | 48 h | | | |
|---|---|---|---|---|---|---|---|---|
| Heating rate (°C/min) | 10 | 20 | 30 | 40 | 10 | 20 | 30 | 40 |
| PLA | 317 | 338 | 345 | 351 | 316 | 335 | 343 | 349 |
| PLA/5col | 330 | 346 | 350 | 360 | 328 | 344 | 348 | 357 |
| PLA/10col | 331 | 349 | 355 | 362 | 330 | 348 | 352 | 359 |
| PLA/5sol | 319 | 340 | 347 | 354 | 317 | 338 | 344 | 351 |
| PLA/10sol | 321 | 343 | 349 | 355 | 319 | 341 | 346 | 353 |

**TABLE II**
**Activation Energy (kJ/mol) of Thermal Degradation from Kissinger and Ozawa Method**

| | Kissinger | | Ozawa (average) | |
|---|---|---|---|---|
| Hydrolysis | 0 h | 48 h | 0 h | 48 h |
| PLA | 167.78 | 153.23 | 159.86 | 148.87 |
| PLA/5col | 187.14 | 167.60 | 181.03 | 170.97 |
| PLA/10col | 215.54 | 186.17 | 194.90 | 177.84 |
| PLA/5sol | 172.08 | 164.77 | 165.11 | 153.86 |
| PLA/10sol | 181.00 | 171.72 | 174.88 | 165.18 |

The activation energy, $E_a$, can be obtained from the slope of a plot of log (against $1/T$ at a specific weight loss, where $T$ is the temperature. Figure 8(a,b) shows the dependence of $E_a$ values on weight loss. It can be seen that the decomposition activation energy increased, and then decreased with increasing weight loss. Presumably, this was due to the changes in mechanism during the thermal decomposition. The average $E_a$ values from Ozawa method are also collected in Table II. The $E_a$ values, at a

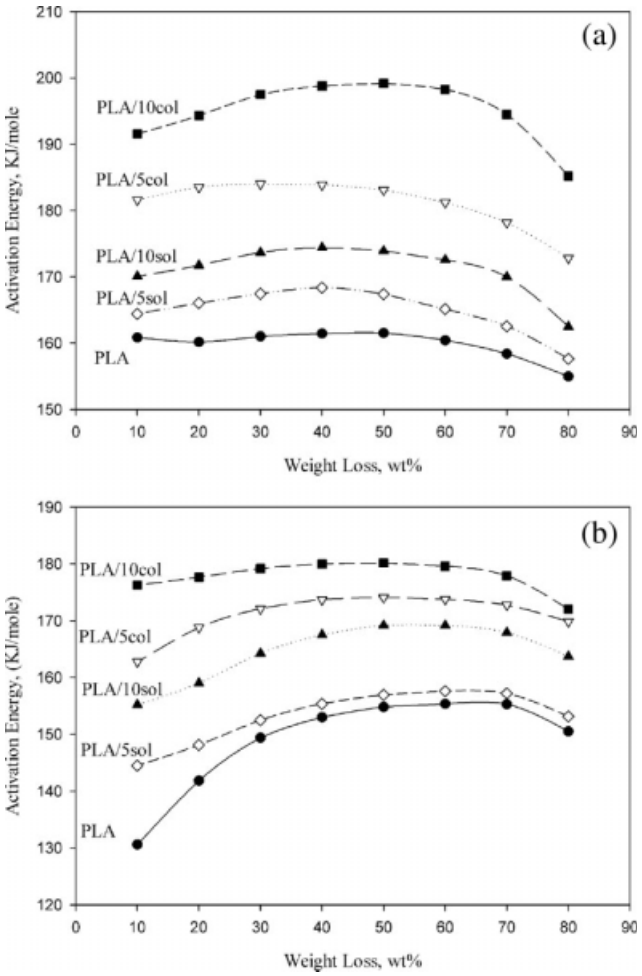


**Figure 8** The dependence of thermal degradation activation energy on weight loss: (a) as prepared and (b) after hydrolysis 48 h.

specific weight loss or average value, follow similar order as those obtained from the Kissinger method.

In the PLA/silica composite films, the presence of silica might alter their thermal degradation process, being compared with neat PLA film. Introducing silica into the PLA resin increases the activation energies of degradation. The thermal resistance of silica will increase the energy demand for thermal degradation of organic resins. It may be attributed to a reduction of molecular mobility and delayed volatilization, which are caused by the silica particles dispersed in the composite films.[34] Liu et al.[35] argued that this effect would be certainly significant because of the low potential energy of surface of silica, resulting in the migration of silica to the surface of resins to form a heat-resistant layer.

## CONCLUSIONS

The PLA/silica composite films with nanosize particles were prepared by blending with colloid silica sol, and microsize particles were prepared by sol–gel method. The nano and microsize silica particles are well dispersed in PLA matrix. The tensile stress, modulus, and thermal stability increases with the addition of silica, even after hydrolysis. The nanosize particles have more notable effects than the micro ones because nanoscale particles provide more area and interaction between the particles and polymer matrix to retard molecular mobility.

## References


1. Ikada, Y.; Tsuji, H. Macromol Rapid Commun 2000, 21, 117.
2. Tsuji, H. In Recent Research Developments in Polymer Science; Pandalai, S. G., Ed.; Transworld Research Network: Trivandrum, India, 2000; Vol. 4, pp 13–37.
3. Mauduit, J.; Perouse, E.; Vert, M. J Biomed Mater Res 1996, 30, 201.
4. Tsuji, H.; Yamada, T.; Suzuki, M.; Itsuno, S. Polym Int 2003, 52, 269.
5. Yoon, J. S.; Lee, W. S.; Kim, K. S.; Chin, I. J.; Kim, M. N.; Kim, C. Eur Polym J 2000, 36, 435.
6. Zhang, L.; Goh, S. H.; Lee, S. Y. Polymer 1998, 39, 4841.
7. Meaurio, E.; Zuza, E.; Sarasua, J. R. Macromolecules 2005, 38, 1207.
8. Gajria, A. M.; Dave, V.; Gross, R. A.; McCarthy, S. P. Polymer 1996, 37, 437.
9. Zhang, G.; Zhang, J.; Wang, S.; Shen, D. J Polym Sci Part B: Polym Phys 2003, 41, 23.
10. Eguiburu, J. L.; Iruin, J. J.; Fernandez-Berridi, M. J.; Roman, J. S. Polymer 1998, 39, 6891.
11. Yuan, Z.; Favais, B. D. Biomaterials 2004, 25, 2161.
12. Yoon, J. S.; Oh, S. H.; Kim, M. N.; Chin, I. J.; Kim, Y. H. Polymer 1999, 40, 2303.
13. Nakamura, T.; Hitomi, S.; Watanabe, S.; Shimizu, Y.; Jamshidi, K.; Hyon, S.-H.; Ikada, Y. J Biomed Mater Res 1989, 23, 1115.
14. Ray, S. S.; Maiti, P.; Okamoto, M.; Yamada, K.; Ueda, K. Macromolecules 2002, 35, 3104.
15. Yan, S. F.; Yin, J. B.; Yang, Y.; Dai, Z. Z.; Ma, J.; Chen, X. S. Polymer 2007, 48, 1688.
16. Wu, L.; Cao, D.; Huang, Y.; Li, B. G. Polymer 2008, 49, 742.
17. Chujo, Y. Curr Opin Solid State Mater Sci 1996, 1, 806.
18. Ahmad, Z.; Mark, J. E. Chem Mater 2001, 13, 3320.
19. Liu, Y. L.; Hsu, C. Y.; Wei, W. L.; Jeng, R. J. Polymer 2003, 44, 5159.
20. Huang, J. W.; Wen, Y. L.; Kang, C. C.; Yeh, M. Y. Polym J 2007, 39, 654.
21. Im, J. S.; Lee, J. H.; An, S. K.; Song, K. W.; Jo, H. J.; Lee, J. O.; Yoshinaga, K. J Appl Polym Sci 2006, 100, 2053.
22. Wang, W.; Ping, P.; Chen, X.; Jing, X. Eur Polym J 2006, 42, 1240.
23. Kubies, D.; Ščudla, J.; Puffr, R.; Sikora, A.; Baldrian, J.; Kovářová, J.; Šlouf, M.; Rypáček, F. Eur Polym J 2006, 42, 888.
24. Peña, J.; Corrales, T.; Izquierdo-Barba, I.; Doadrio, A. L.; Vallet-Regí, M. Polym Degrad Stab 2006, 91, 1424.
25. Saha, S. K.; Tsuji, H. Polym Degrad Stab 2006, 91, 1665.
26. Tsuji, H.; Mizuno, A.; Ikada, Y. J Appl Polym Sci 1998, 70, 2259.
27. Tsuji, H. Biomaterials 2003, 24, 537.
28. Wu, D.; Wu, L.; Wu, L.; Zhang, M. Polym Degrad Stab 2006, 91, 3149.
29. Chang, J. H.; An, Y. U.; Sur, G. S. J Polym Sci Part B: Polym Phys 2003, 41, 94.
30. Ogata, N.; Jimenez, G.; Kawai, H.; Ogihara, T. J Polym Sci Part B: Polym Phys 1997, 35, 389.
31. Tsuji, H.; Kawashima, Y.; Takikawa, H.; Tanaka, S. Polymer 2007, 48, 4213.
32. Kissinger, H. E. Anal Chem 1957, 29, 1702.
33. Ozawa, T. A. Bull Chem Soc Jpn 1965, 38, 1881.
34. Gilnian, J. W.; Kashivagi, T. C. L.; Giannelis, E. P.; Manias, E.; Lomakin, S.; Lichtenhan, J. D.; Jones, P. In Fire Retardancy of Polymers; Le Bras, M.; Caniino, G.; Bourbigot, S.; Delobel, R., Eds.; Royal Society of Chemistry: Cambridge, England, 1998.
35. Liu, Y. L.; Wei, W. L.; Hsu, K. Y.; Ho, W. H. Thermochim Acta 2004, 412, 139.